SSRG International Journal of Electrical and Electronics Engineering
ISSN: 2348-8379/ https://doi.org/10.14445/23488379/IJEEE-V10I8P110

Volume 10 Issue 8, 102-111, August 2023

Original Article

A 3.5 GHz Band RF Wireless Signal Transmission Mechanism in Various Aqueous Solutions

Koyu Chinen[1], Ichiko Kinjo[2]

[1]*GLEX, Yokohama, Japan.*
[2]*Department of Information Communication System Engineering, National Institute of Technology, Okinawa College, Okinawa, Japan.*

[1]*Corresponding Author : koyu.chinen@nifty.com*

Received: 10 June 2023 Revised: 14 July 2023 Accepted: 09 August 2023 Published: 31 August 2023

Abstract *- We investigated RF-band wireless transmission characteristics in aqueous solutions by evaluating S-parameters. Different solutions of pure water, NaCl, alcohol, and IPA were filled into a 250 mm long ABS resin capsule terminated with 50 Ω SMA electrodes. The S-parameters of S_{11} and S_{21} were measured in the frequency range from 0.1 to 7 GHz using a Vector Network Analyzer (VNA). The frequency measured at the minimum value of the S_{11} is approximately 3.5 GHz, which is the frequency at which most of the maximum values of S_{21} were measured for the different solutions and were determined by the SMA electrode structure. When a magnetostatic or an electrostatic field was applied externally to the capsule and the mechanical shape of the capsule was changed, the changes in the S-parameter of S_{21} were evaluated. We clarified that the drift, rotation, and vibration of the protonic polar molecules of H_2O dominate the transmission of the RF wireless signal in the aqueous solutions, and the impedance matching between the SMA electrode and pure water determines the transmission frequency.*

Keywords *- Solution RF-wireless communication, Underwater wireless communication, S-parameter, VNA, Polar molecule water.*

1. Introduction

Wireless signal transmission using electromagnetic waves is one of the most promising communication methods in seawater and freshwater, and there have been many reports about research in this area. [1-17] However, the propagation mechanism of RF-band electromagnetic waves in aqueous solution is still0020largely unknown. In this study, we investigated the electrical mechanism of the RF wireless signal propagations in the different types of solutions and the effects of applying a magnetostatic field and changing the shape of the solution capsule. For this purpose, we evaluated Scattering (S) parameters describing the transmission characteristics of the RF wireless signals in aqueous solutions using a vector network analyzer to measure the transmission coefficients S_{21} and reflection coefficients S_{11} of the S-parameters. [18-20] We focused our analysis on the role of protonic polar molecules H_2O in aqueous solutions in the propagation of RF wireless signals.

2. S-parameter Measurements for RF Wireless Signal Transmissions in Aqueous Solutions

We evaluated the reflection and transmission signals by inputting square-wave RF signals with a frequency range of 0.1-7 GHz to the aqueous solutions to measure the transmission coefficients S_{21} and the reflection coefficients S_{11}. [18-20] The aqueous solutions were filled into Acrylonitrile Butadiene Styrene (ABS) resin capsule with an inner diameter of 8 mm and a length of 250 mm. [21, 22] Sub Miniature Type A (SMA) electrodes with an impedance of 50 Ω were attached to the input and output ends of the resin capsules. The SMA input electrode was connected to the output port of the vector network analyzer with a 50 Ω coaxial cable, and the output electrode of the resin capsule was connected to a 20dB gain and 0.1-7 GHz wide-band Low-Noise Amplifier (LNA) fabricated with a single-stage SiGe bipolar transistor. The output of the LNA was connected to the input port of the vector network analyzer. The configuration of this S-parameter measurement setup is illustrated in Figure 1.

3. S-parameter Measurements Results for RF Wireless Signal Transmission in Aqueous Solutions

We measured the S-parameters of the RF wireless signal transmissions using a solution capsule filled with pure water refined by an ion-exchange resin and reverse osmosis.

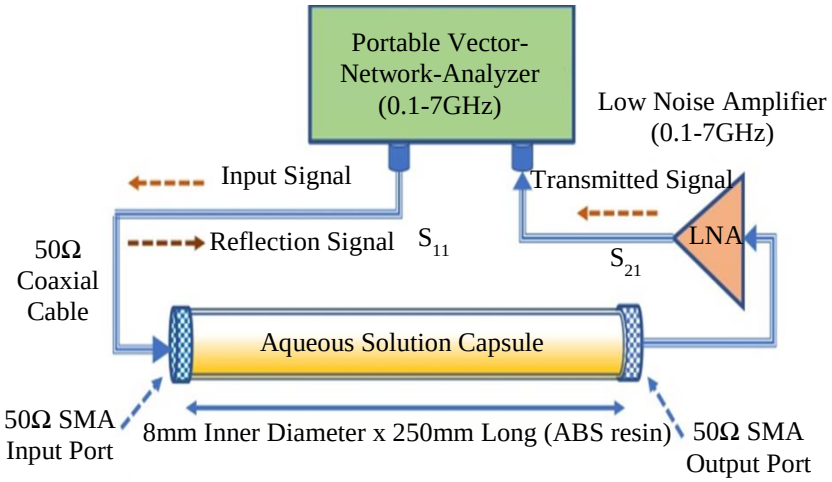

Fig. 1 Configuration of S-parameter measurement setup for RF wireless

The measurement result is shown in Figure 2. The result measured for a hollow (air) resin capsule is also shown for comparison. The curve of the reflection coefficient S_{11} for pure water shows a dip at a frequency of about 3.5 GHz, indicating that the SMA input electrode and the pure water are relatively electrically matched at a frequency of about 3.5 GHz. Two significant peaks appear in the curve of the transmission coefficient S_{21} measured for pure water.

The peak in the low-frequency range below 2 GHz represents the signals transmitted through the resin capsule (ABS enclosure). [23-26] When the resin capsule was hollow (air), the peak of the S_{21} curve in the low-frequency range significantly decreased because the signal path of pure water was eliminated from a series of the signal conduction paths: SMA input electrode ⇒ pure water ⇒ ABS resin enclosure ⇒ pure water ⇒ SMA output electrode. The decrease in the value of S_{21} at frequencies lower than 1 GHz was due to the decrease in the gain at low frequencies of the LNA.

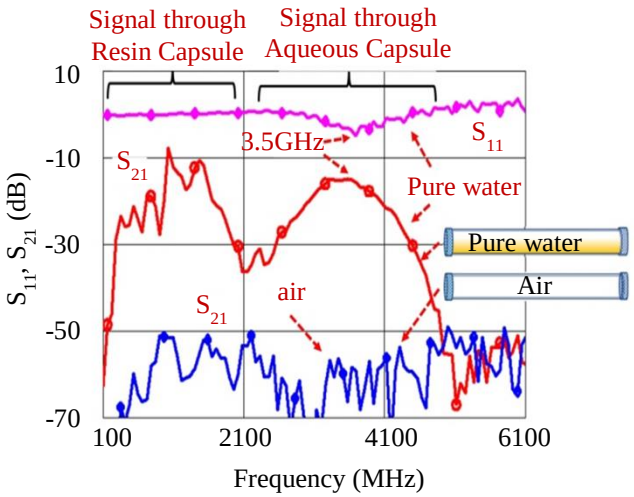

Fig. 2 Reflection coefficients S_{11} and transmission coefficients S_{21} were measured for pure water and air filled in the capsules

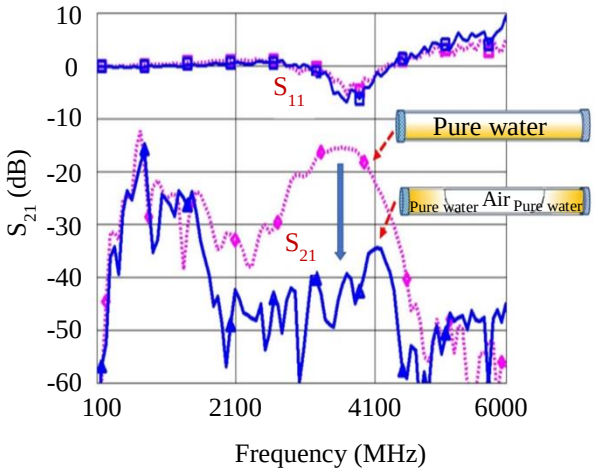

Fig. 3 Reflection coefficients S_{11} and transmission coefficients S_{21} were measured for pure water and partially filled with air in the capsules

Figure 3 shows the S_{21} measurement results when only the space around the transmitter and receiver electrodes in the capsule was filled with pure water, and the intermediate space between the transmitter and receiver electrodes was air. Compared to the case where the entire capsule was filled with pure water, S_{21} around 3.5 GHz was significantly reduced.

However, the S_{21} value below 2 GHz was almost unchanged. This result indicates that signals in the low-frequency range below 2 GHz are transmitted through the resin envelope of the capsule, a solid dielectric material, via the pure water around the electrodes. If there is no pure water around the electrode, signals below 2 GHz are not transmitted to the resin envelope of the capsule.

Immersion of the electrode in pure water allows the transmission and reception of high-frequency signals, but the electrode alone cannot transmit or receive high-frequency signals. The SMA electrode structure is impedance-matched

to pure water at specific frequencies within the measurement frequency and mismatched to air. Signals at frequencies from 2 to 5 GHz in the curve of S_{21} show the signals transmitted through pure water in the capsule. Therefore, this study focused on the signals measured in the high-frequency range above 2 GHz to analyze the transmission coefficients S_{21} for the aqueous solutions.

4. RF Wireless Signal Propagation Mechanism in Salty Aqueous Solutions

Many types of aqueous solutions contain ionized atoms from solutes. To investigate the role of these ions in the RF wireless signal propagation, we measured the S-parameters for aqueous solutions of NaCl which has a high solubility in water.[18, 27] The values of the transmission coefficient S_{21} measured for different molar concentrations of NaCl are shown in Figure 4.

The values of S_{21} decreased with increasing NaCl molar concentration. At a concentration of 0.5 mol/L, the value of S_{21} decreased more than 10 dB than that of pure water. Since the molar concentration of NaCl in seawater is approximately 0.53 mol/L, the attenuation rate of the RF wireless signal propagation in the seawater is higher than that in freshwater. [9] Any concentration dependence of the NaCl solution did not appear for the curves of S_{21} measured below 2 GHz because the signals in the frequency range below 2 GHz were transmitted through the outer ABS resin capsule.

As shown in Figure 5, the RF wireless signals in the solutions of NaCl are propagated by the vibration and rotation of polar molecule H_2O and the release and combination of the protons and electrons. [18] The ions of Na^+ and Cl^- bound to the polar molecule H_2O become hydrated ions and do not contribute to the propagation of the RF wireless signals in the GHz frequency range because of their considerable molecular weight.

In addition, the hydrated ions and molecule H_2O bound to the ions are obstacles to the vibration and rotation of unbounded polar molecule H_2O and collisions. Therefore, the transmission coefficients S_{21} decreased with increasing NaCl concentration

At low frequencies below 100 MHz, the transmission coefficient S_{21} increases with decreasing frequency as the NaCl concentration increases. Because the hydrated ions of Na^+ and Cl^- bound to the polar molecule H_2O can follow the change in the electric field at low frequencies. [18] However, when the concentration of NaCl exceeds a high value of about 0.1 mol/L, the value of S_{21} saturates and then decreases with the NaCl concentration. [18] At the low frequencies, an increase in the frequency of collisions between the hydrated ions of Na^+ and Cl^- with increasing the NaCl concentration is considered.

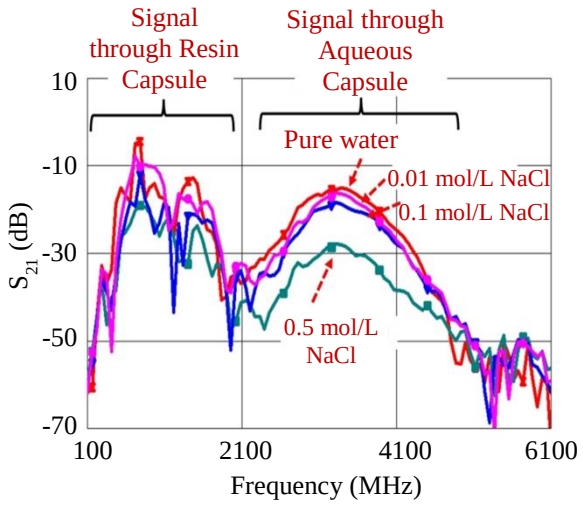

Fig. 4 Transmission coefficients S_{21} were measured for different NaCl concentration aqueous solutions

5. RF Wireless Signal Propagation Mechanism in Alcoholic Aqueous Solution

Protonic polar molecules such as water H_2O, methanol, ethanol, and 2-propanol (IPA) have high relative permittivity ε_r, solubility parameter δ, and polarity parameter P', as shown in Table 1. [29-31] Since the water H_2O is a unique solvent with the highest values of these polarity parameters, we focused on its role in the RF wireless signal propagations.

The S-parameter transmission coefficients S_{21} were evaluated to investigate the propagation characteristic of the RF wireless signals in aqueous alcohol solutions with different compositions and concentrations. The measured transmission coefficients of S_{21} decreased with increasing alcohol concentration, as shown in Figure 6.

The value of S_{21} for 99.5% ethanol and 99.5% IPA is about 20 dB lower than that of pure water. As shown in Table 1, the contribution of the alcohol polar molecules to the transmission coefficients S_{21} of the RF wireless signals is small because alcohol has low relative permittivity and polarity parameters. Therefore, the transmission of the RF wireless signals in aqueous alcohol solutions is primarily dominated by the vibration and rotation of the polar molecule H_2O and by the release and binding of protons H^+ and electrons e^-.

Since IPA has the lowest polarity parameter value, the transmission coefficient S_{21} shows the lowest value. The S_{21} curve of the IPA solution in the low-frequency range below 2 GHz represents the transmission coefficient measured for a series of the signal conduction paths: SMA input electrode ⇒ IPA ⇒ ABS resin capsule ⇒ IPA ⇒ SMA output electrode. Therefore, the value of S_{21} shows the lowest because the signal passes through IPA, which has the lowest polarity parameter.

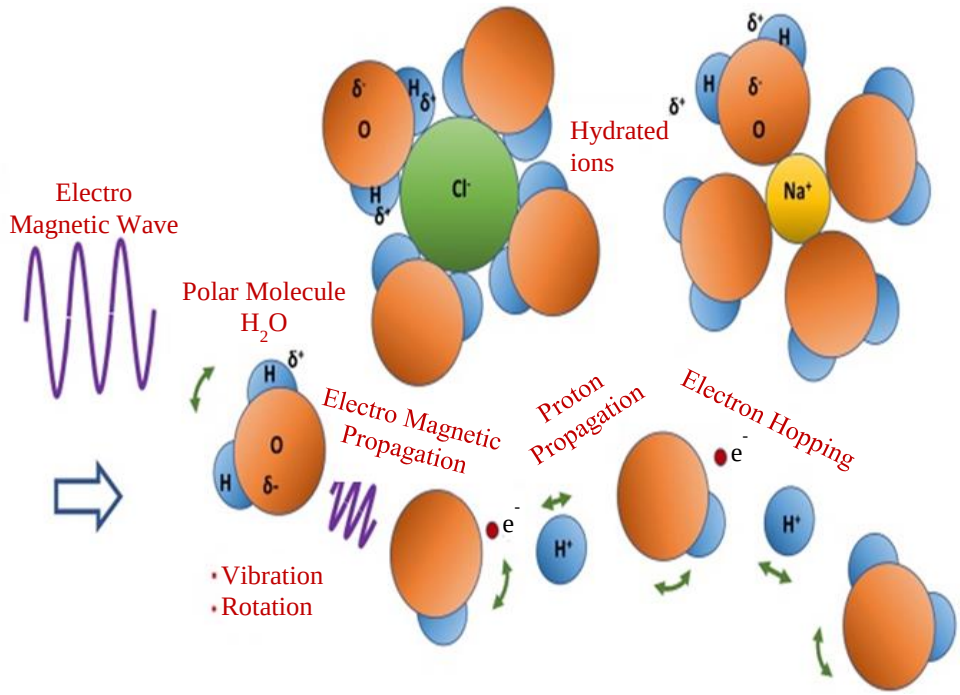

Fig. 5 Propagation mechanism illustrated for RF signal in a NaCl aqueous solution

Table 1. Electrochemical properties of protic polar molecules [29]

Solvent	Chemical formula	Formula weight	ε_r	Solubility (δ)	Polarity (P')
Water	H_2O	18.02	78.5	21.0	10.2
Methanol	CH_3OH	32.04	32.6	12.9	5.1
Ethanol	C_2H_5OH	46.07	24.6	11.2	4.3
IPA	C_3H_7OH	60.1	18.3	10.2	3.9

At low frequencies below 100 MHz, the value of the transmission coefficient S_{21} for IPA is the smallest among solutions of NaCl, ethanol, and IPA because IPA has primarily no contributions of ionic conduction to the signal propagation. [18] Therefore, ethanol and IPA are not suitable solvents for RF wireless signal transmissions.

A shielding effect can be expected for high-frequency signals.Values of the transmission coefficient S_{21} measured at a frequency of 3.4 GHz for different concentrations of salt water, aqueous alcohol solution, and drinking water are shown in Figure 7.

The values of transmission coefficient S_{21} decreased significantly when the concentration of NaCl exceeded 0.1 mol/L and the alcohol concentration exceeded 15 %. Since seawater has a salinity of about 0.53 mol/L, the value of S_{21} is about 10 dB lower than freshwater. Tap water, mineral water, and saltwater with a concentration of NaCl less than 0.001 mol/L are suitable for the RF wireless signal propagations since the transmission coefficients S_{21} for these solutions are comparable to these of pure water.

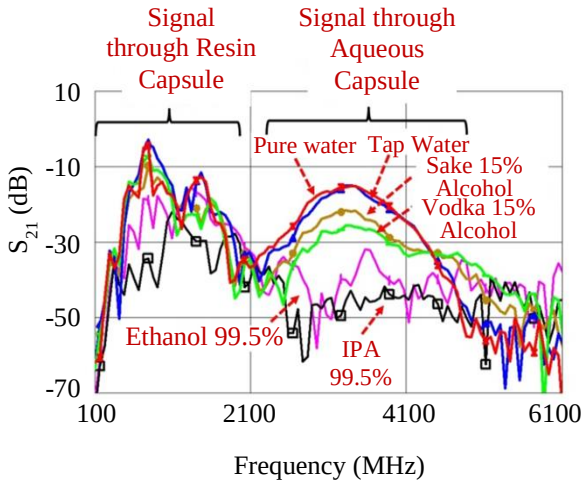

Fig. 6 Transmission coefficients S_{21} were measured for different alcohol aqueous solutions

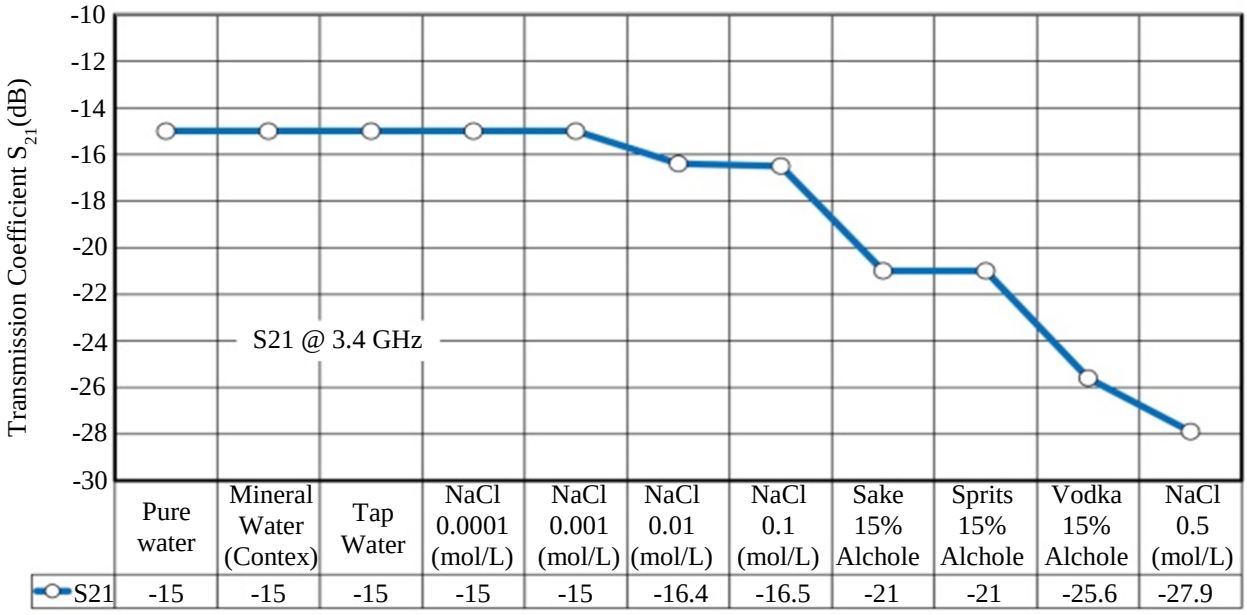

Fig. 7 Transmission coefficients S_{21} were measured for different aqueous solutions at a frequency of 3.4 GHz

6. RF Wireless Signal Reflection Characteristics of Aqueous Solutions

Figure 8 shows measured reflection coefficients S_{11} of the RF wireless signals in the NaCl aqueous solutions. Since the aqueous NaCl solution is considered, such as a dielectric, the curve of S_{11} is plotted on the admittance Smith chart. [18] The conductance *G* increases proportionally to the NaCl concentration in the low-frequency range. In the high-frequency range of the curve of S_{11}, the value of S_{11} measured at a frequency of around 3.5 GHz is relatively close to the 50 Ω impedance. Therefore, the characteristic of S_{11} of the NaCl solution reflects the pure water.

Pure water mainly dominates the RF wireless signal transmission in the NaCl solution. The characteristics of S_{11} of the pure water are determined by the frequency characteristics of vibrating and rotating polar molecules of H_2O and the release and binding of the protons H^+ and electrons e^-, as well as that of the structure of the SMA electrode. In the frequency range for this experiment, the value of 3.5 GHz in the curve of S_{11} was primarily dependent on the design of the SMA electrode because the particular value of 3.5 GHz was measured when the NaCl concentration was varied. Figure 9 shows the reflection coefficients S_{11} of the RF wireless signal measured for the aqueous alcohol solutions and IPA. Since the aqueous alcohol solutions are considered, such as dielectrics, the measured values of S_{11} are plotted on the Smith admittance chart. In the low-frequency range, the aqueous alcohol solutions have very small conductance G because the solutions do not contain ionic molecules such as NaCl that contribute to the conductance G.

In the high-frequency region of the curves of S_{11}, the value of S_{11} measured at 3.5 GHz is primarily close to 50 Ω impedance. Therefore, the curve of S_{11} of the aqueous alcohol solution reflects the S_{11} characteristic of pure water. The susceptance *B* of the aqueous alcohol solutions is similar to that of a dielectric capacitor for the frequency response. Unlike aqueous alcohol solutions, the conductance G of IPA increases in the low-frequency range and becomes constant at a frequency of around 3.5 GHz. The susceptance *B* of IPA is similar to that of a capacitor with a small dielectric for the frequency response. Unlike water and alcohol solutions, IPA does not propagate the RF wireless signals through polar molecules, therefor the low value of *B* represented in the curve of S_{11} and the low values of S_{21} measured (see Figure 6) are in agreement.

A value of 3.5 GHz was observed in the high-frequency range in the S_{11} curves, which is relatively close to an impedance of 50 Ω for the NaCl and aqueous alcohol solutions. This particular value of 3.5 GHz was not significantly affected by the concentration or composition of the aqueous solutions. Therefore, the value of 3.5 GHz was mainly determined by the SMA electrode structure. The reflection coefficient S_{11} was calculated by electromagnetic simulation using a model in which the signal pin of the SMA electrode is surrounded by pure water. The signal pin is made of copper and has a diameter of 1 mm and a length of 4 mm. The electromagnetic simulator used was AXIEM. [32] Figure 10 shows the Smith chart representation of the simulation results and the measured values, and Figure 11 shows the Cartesian coordinate representation and the current density distribution simulated.

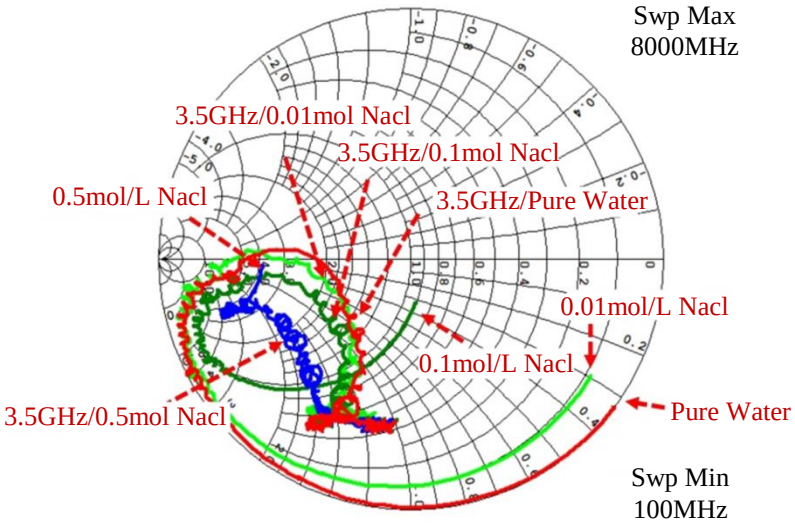

Fig. 8 Reflection coefficients S_{11} were measured for different NaCl concentration aqueous solutions

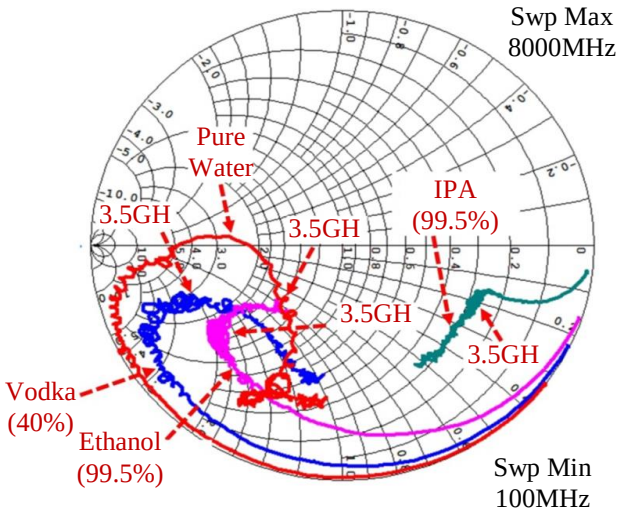

Fig. 9 Reflection coefficients S_{11} were measured for different alcohol solutions and IPA

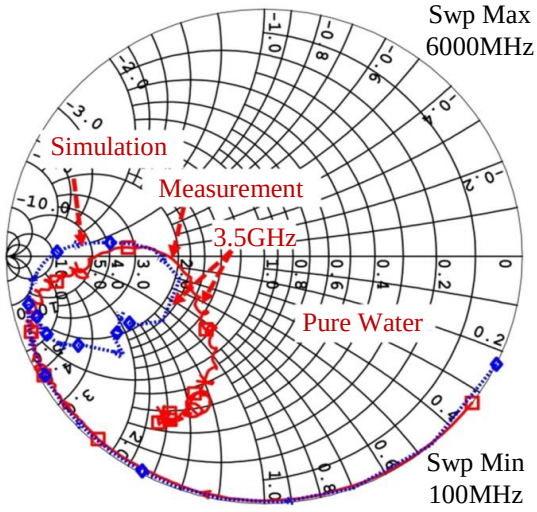

Fig. 10 Reflection coefficients S_{11} were measured and simulated for pure water plotted on the Smith chart

The current density distribution is shown at 3.5 GHz. The current is concentrated on the signal pin's ground, similar to the current density distribution of a grounded monopole antenna. However, the difference between the measured and simulated values is more significant at higher frequencies. This result may be because the actual SMA electrode structure is rather complex, while the simulation model is simplified.

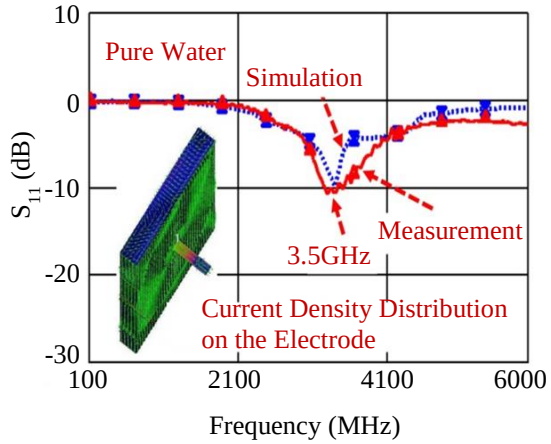

Fig. 11 Reflection coefficients S_{11} measured and simulated for pure water and plotted on cartesian coordinates, and an illustration of current density distribution on the SMA electrode is represented

7. Change in RF Wireless Signal Propagation Characteristics with Magnetostatic and Electrostatic Field and Capsule Shape

The RF wireless signals in the aqueous solution were propagated mainly by the vibration and rotation of the polar molecule H_2O and the release and binding of protons H^+ and electrons e^-. To confirm it, we applied an external magnetostatic field to the solution to constrain the rotation of the polar molecules H_2O and lower the transfer coefficient S_{21}. The applied magnetostatic field was generated by placing sixteen magnets with a magnetic flux density of 60 mT /magnet at the bottom of the capsule. The applied magnetostatic field area was approximately 145 mm long, as shown in Figure 12. An electrostatic generated with other ground voltage was applied similarly. The measurement result is shown in Figure 13. The decrease in the value of S_{21} was due to the application of magnetostatic and electrostatic fields. Hence the RF wireless signals are propagated by changes in the electric and magnetic fields in the solution.

The measured values S_{21} show a spectrum with several significant dips. Possible causes of these dips include multiple reflections at the boundary between the magnetostatic field-applied and non-applied regions in the longitudinal direction within the aqueous solution capsule.In the low-frequency range below 2 GHz, there was almost no decrease in S_{21} for the RF signal propagating through the capsule enclosure. External magnetostatic and electrostatic fields do not affect signal transmission in the capsule enclosure. This result is considered a different mode of RF signal transmission in solid dielectric material from that of electromagnetic wave propagation in aqueous solution. This transmission mode differs from electromagnetic wave propagation in an aqueous solution. [23-26]

Change in the length and shape of the aqueous solution capsule was considered to alter the signal transmission characteristic of the polar molecule H_2O. Doubling the length of the capsule reduced the transmission coefficient of S_{21} by about 5 dB when measured for the peak value of S_{21} at 3.3 GHz (Figure 14), and bending the capsule into an L-shape lowered the value of S_{21} by about 7 dB (Figure 15 and 16). The capsule has a tubular cylindrical shape. Therefore, the direction of vibration and rotation of the polar molecule H_2O determine the direction of the RF wireless signal transmission.

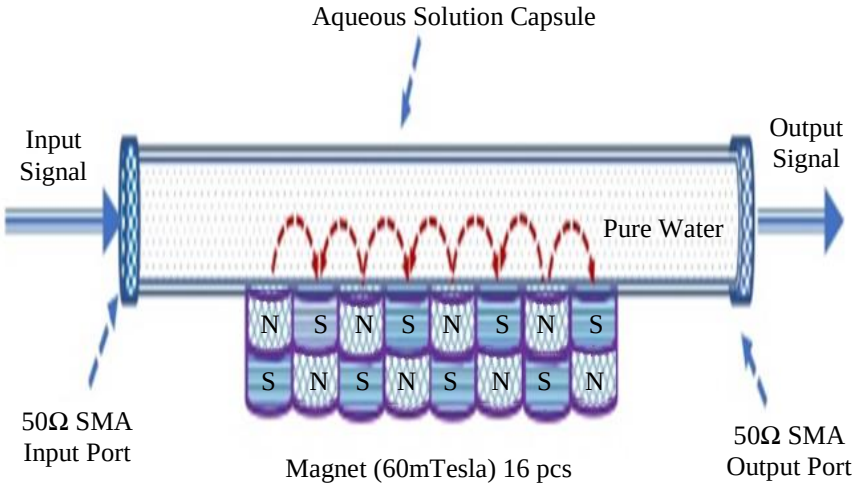

Fig. 12 A magnetostatic field was applied to the resin capsule using a setup

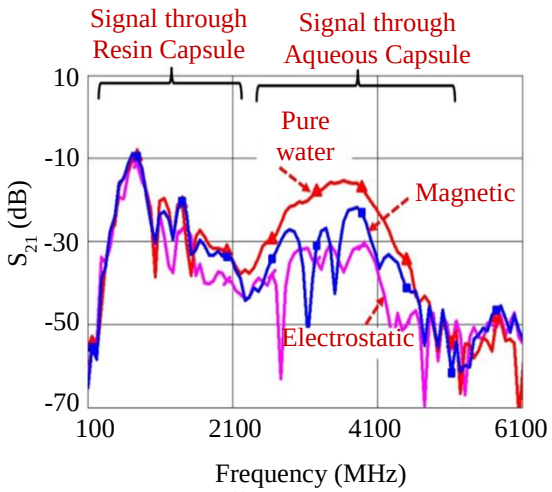

Fig. 13 Transmission coefficients S_{21} were measured when the magnetostatic field was applied to the resin capsule

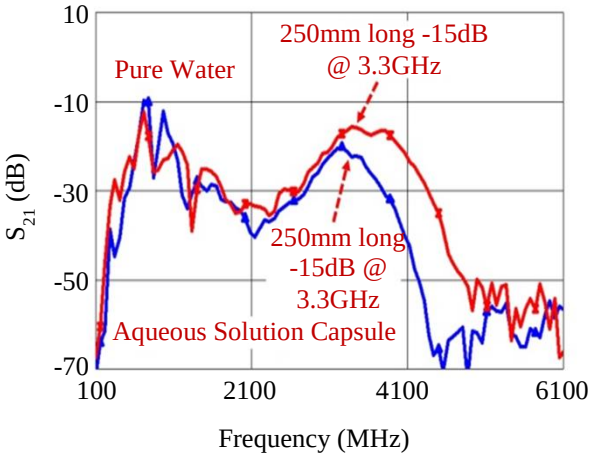

Fig. 14 Transmission coefficients S_{21} were measured for different aqueous capsule lengths

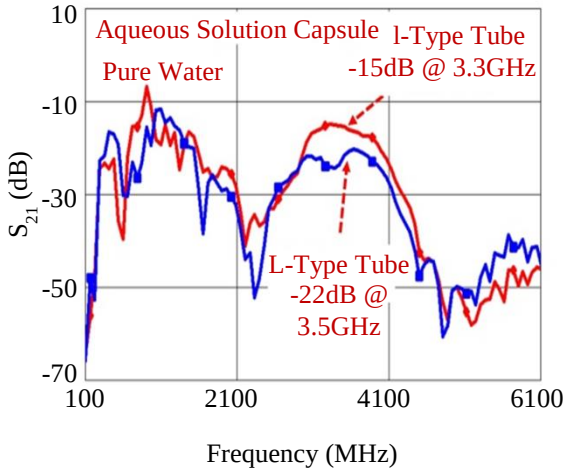

Fig. 15 Transmission coefficients S_{21} were measured for different shapes

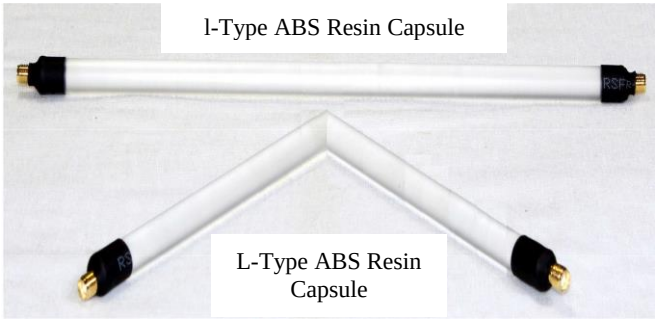

Fig. 16 A photograph of aqueous capsules for different mechanical shapes

8. Conclusion

We analyzed the transmission characteristics of the RF wireless signals in aqueous solutions containing polar molecule H_2O by measuring the S-parameters for a frequency range of 0.1-7 GHz using a vector network analyzer. In aqueous solutions with different NaCl concentrations, the transmission coefficient S_{21} decreased significantly at salinities above 0.1 mol/L. In aqueous alcohol solutions, the value of S_{21} decreased significantly when the alcohol concentration increased by more than 15%. Therefore, we clarified that the RF wireless signals are mainly transmitted by polar molecules H_2O.

When we measured the reflection coefficient of S_{11}, the conductance of G increased with increasing salinity in the low-frequency range, and the curve of S_{11} was close to an impedance of 50 Ω at 3.5 GHz in the high-frequency range. For alcohol solutions, the curves of S_{11} around 3.5 GHz were close to an impedance of 50 Ω. The transmission coefficient S_{21} of the RF wireless signal reaches its maximum value at a frequency, and the frequency does not depend on the solvents. Hence, we clarified that the SMA electrode structure mainly determines the impedance matching frequency. Because the transmission coefficients S_{21} of the RF wireless signals decreased significantly when the magnetostatic or electrostatic fields were applied to aqueous solutions, we clarified that the RF wireless signals in the aqueous solution are transmitted by changes in the electric and magnetic fields, such as electromagnetic waves.

Because the transmission coefficient S_{21} of the RF wireless signal changed with changes in the shape of the solution capsule, we clarified that the RF wireless signal propagated along the direction of the changes in the electromagnetic field caused by the vibration and rotation of the neighbouring polar molecule H_2O. This research can be applied to RF wireless signal communication in aqueous solutions, RF signal communication between high-voltage devices, EMC reduction, detection of NaCl concentration, detection of alcohol concentration, solutions and bio-tissue analysis, monitoring of pure water purification equipment, and detection of external magnetic and electric fields.

References

[1] Xianhui Che et al., "Re-Evaluation of RF Electromagnetic Communication in Underwater Sensor Networks," *IEEE Communications Magazine*, vol. 48, no. 12, pp. 143-151, 2010. [CrossRef] [Google Scholar] [Publisher Link]

[2] Brian Kelley, Kranthi Manoj, and Mo Jamshidi, "Broadband RF Communications in Underwater Environments using Multi-Carrier Modulation," *2009 IEEE International Conference on Systems, Man and Cybernetics*, San Antonio, USA, pp. 2303-2308, 2009. [CrossRef] [Google Scholar] [Publisher Link]

[3] Caroline Peres et al., "Theoretical Models for Underwater RFID," *The Thirteenth International Conference on Sensor Technologies and Applications*, Nice, France, pp. 80-88, 2019. [CrossRef] [Google Scholar] [Publisher Link]

[4] Hongfa Zhao et al., "Underwater Wireless Communication via TENG-Generated Maxwell's Displacement Current," *Nature Communications*, vol. 13, no. 1, p. 3325, 2022. [CrossRef] [Google Scholar] [Publisher Link]

[5] Igor Smolyaninov, Quirino Balzano, and Dendy Young, "Development of Broadband Underwater Radio Communication for Application in Unmanned Underwater Vehicles," *Journal of Marine Science and Engineering*, vol. 8, no. 5, pp. 1-10, 2020. [CrossRef] [Google Scholar] [Publisher Link]

[6] Irene Cappelli et al., "Underwater to above Water LoRa Transmission: Technical Issues and Preliminary Tests," *22nd International Workshop on ADC and DAC Modelling and Testing*, pp. 96-101, 2020. [Google Scholar] [Publisher Link]

[7] Jun Wang, and Shilian Wang, "Seawater Short-Range Electro-Magnetic Wave Communication Method Based on OFDM Subcarrier Allocation," *Journal of Computer and Communications*, vol. 7, no. 10, pp. 63-71, 2019. [CrossRef] [Google Scholar] [Publisher Link]

[8] Muhammad Rauf et al., "Surface Waves Analysis of Efficient Underwater Radio-Based Wireless Link," *Mathematical Problems in Engineering*, vol. 2021, pp. 1-10, 2021. [CrossRef] [Google Scholar] [Publisher Link]

[9] Kenechi G. Omeke et al., "Characterization of RF Signals in Different Types of Water," *Antennas and Propagation Conference 2019*, Birmingham, UK, pp. 1-6, 2019. [CrossRef] [Google Scholar] [Publisher Link]

[10] Suresh Kumar, and Chanderkant Vats, "Underwater Communication: A Detailed Review," *WCNC-2021: Workshop on Computer Networks and Communications*, pp. 76-86, 2021. [Google Scholar] [Publisher Link]

[11] Mohammad Tariqul Islam et al., "Detection of Salt and Sugar Contents in Water on the Basis of Dielectric Properties using Microstrip Antenna-Based Sensor," *IEEE Access*, vol. 6, pp. 4118-4126, 2018.[CrossRef] [Google Scholar] [Publisher Link]

[12] Gyan Raj Koirala et al., "Radio Frequency Detection and Characterization of Water-Ethanol Solution through Spiral-Coupled Passive Micro-Resonator Sensor," *Sensors*, vol. 18, no. 4, pp. 1-10, 2018.[CrossRef] [Google Scholar] [Publisher Link]

[13] H. P. Schwan, and K. R. Foster, "Microwave Dielectric Properties of Tissue, some Comments on the Rotational Mobility of Tissue Water," *Biophysical Journal*, vol. 17, pp. 193-197, 1977. [CrossRef] [Google Scholar] [Publisher Link]

[14] Mohd Aziz Aris et al., "Microwave Characterization of Pandanus Atrocarpus as Potential Organic-Based Dielectric Substrate," *International Journal of Electrical and Computer Engineering*, vol. 12, no. 4, pp. 3792-3799, 2022. [CrossRef] [Google Scholar] [Publisher Link]

[15] E. M. Cheng et al., "Development of Microstrip Patch Antenna Sensing System for Salinity and Sugar Detection in Water," *International Journal of Mechanical and Mechatronics Engineering*, vol. 14, no. 5, pp. 31-36, 2014. [Google Scholar] [Publisher Link]

[16] Smita L. Baikar, S. S. Thakur, and V. C. Kshirsagar, "Printed Ring Monopole Antenna for Medical Application," *Journal of Emerging Technologies and Innovative Research*, vol. 6, no. 5, pp. 747-750, 2019. [Publisher Link]

[17] Yujian Li, and Kwai-Man Luk, "A Water Dense Dielectric Patch Antenna," *IEEE Access*, vol. 3, pp. 274-280, 2015. [CrossRef] [Google Scholar] [Publisher Link]

[18] Koyu Chinen, Shoko Nakamoto, and Ichiko Kinjo, "Two-Port Equivalent Circuits Deduced from S-Parameter Measurements of NaCl Solutions," *IETE Journal of Research*, 2022. [CrossRef] [Google Scholar] [Publisher Link]

[19] Sonia Sindhu, "Multi-Hop Data Communication for Cluster Based Wireless Sensor Networks: A Review," *International Journal of Computer & Organization Trends*, vol. 6, no. 2, pp. 4-6, 2016. [CrossRef] [Publisher Link]

[20] Andrew Horsley, and David S. Thaler, "Microwave Detection and Quantification of Water Hidden in and on Building Materials: Implications for Healthy Buildings and Microbiome Studies," *BMC Infectious Diseases*, vol. 19, no. 67, pp. 1-8, 2019. [CrossRef] [Google Scholar] [Publisher Link]

[21] Omnexsus, Comprehensive Guide on Acrylonitrile Butadi-ene Styrene (ABS). [Online]. Available: https://omnexus.specialchem.com/selection-guide/acrylonitrile-butadiene-styrene-abs-plastic

[22] Acrylonitrile-Butadiene-Styrene (ABS) - Polymer Database. [Online]. Available: https://polymerdatabase.com/CommercialPolymers/ABS.html

[23] Ha Il Song, Huxian Jin, and Hyeon-Min Bae, "Plastic Straw: Future of High-Speed Signaling," *Scientific Reports*, vol. 5, pp. 1-8, 2015. [CrossRef] [Google Scholar] [Publisher Link]

[24] R. Karthika, and S. Balakrishnan, "Wireless Communication using Li-Fi Technology," *SSRG International Journal of Electronics and Communication Engineering*, vol. 2, no. 3, pp. 7-14, 2015. [CrossRef] [Google Scholar] [Publisher Link]

[25] Ha Il Song et al., "E-Tube: Dielectric Waveguide Cable for High-Speed Communication," *Scientifc Reports*, vol. 10, pp. 1-8, 2020. [CrossRef] [Google Scholar] [Publisher Link]

[26] Satoshi Kodama, and Sari Nagao, "Application of Existing Network Methods in Low Power Long Range Wireless Communication," *International Journal of P2P Network Trends and Technology*, vol. 10, no. 1, pp. 1-9, 2020. [CrossRef] [Google Scholar] [Publisher Link]

[27] N. D. Pavlov, and Y. A. Baloshi, "Electromagnetic Properties of Water on GHz Frequencies for Medicine Tasks and Metamaterial Applications," *Journal of Physics: Conference Series*, vol. 643, no. 1, pp. 1-5, 2015. [CrossRef] [Google Scholar] [Publisher Link]

[28] Maria Ekimova et al., "From Local Covalent Bonding to Extended Electric Field Interactions in Proton Hydration," *Journal of the German Chemical Society*, vol. 61, no. 46, pp. 1-9, 2022. [CrossRef] [Google Scholar] [Publisher Link]

[29] Sodex, Polarities of Solvents. [Online]. Available: https://www.shodex.com/en/dc/06/0117.html

[30] S. Murov, Solvent Polarity Table. [Online]. Available: http://murov.info/orgsolvsort.htm

[31] Not Voodoo X.4, Solvents and Polarity. [Online]. Available: https://www.chem.rochester.edu/notvoodoo/pages/reagents.php/page-solvent-polarity

[32] AWR Axiem Planar 3D System Analysis Datasheet. [Online]. Available: https://www.cadence.com/content/dam/cadence-www/global/en_US/documents/tools/system-analysis/rf-microwave-design/AWR_axiem_planar_3D_analysis_ds.pdf